A JEM–X CATALOG OF X–RAY SOURCES

Niels J. Westergaard, Jérôme Chenevez, Niels Lund, Carl Budtz–Jørgensen, and Søren Brandt

Danish National Space Center, Juliane Maries Vej 30, Copenhagen, Denmark

ABSTRACT

The JEM–X catalog of X-ray sources presented here is based on detections in individual science windows with a sensitivity limit of about 10 mCrab (5 – 15 keV). It contains 127 sources and only those that can be identified from the existing reference catalog. The input data are taken from the, up to now, ∼300 INTEGRAL orbits with public data.

Key words: JEM–X; X-ray source catalog.

1. INTRODUCTION

The search for sources has been performed in images from individual pointings (Science Windows). Extracting sources from mosaic images and thereby obtaining better sensitivity for persistent sources is the goal of ongoing activities and has so far led to the discovery of three new X-ray sources [1, 2, 3].

Both JEM–X [4] instruments have been used, JEM–X2 through INTEGRAL revolutions 39 – 170 and JEM–X1 from 170 to 326 (with some exceptions, see later). A large part of the sky is covered as illustrated in Fig. 1 which is a map of the combined exposure time.

The image reconstruction process includes a backprojection method taking into account a detailed model of the instrument and then an IROS (Iterative Removal Of Sources) algorithm for finding weaker sources.

In spite of the effort to exclude spurious sources automatically a number of these will appear in the list of sources. The most efficient way of removing those is to demand that the source should exist in a reference catalog of X-ray sources and here we have used version 25 of the INTEGRAL General Reference Catalog [5].

The JEM–X catalog itself is given in table 1 on the last page of this paper and the explanations for the columns are given immediately before the table.

The 2nd IBIS/ISGRI soft gamma-ray survey catalog [6] contains about 200 sources. There are more sources because the ISGRI FOV is much larger than the JEM–X FOV and the collecting area is also larger. The sources seen by JEM–X but not reported in [6] are marked (†) in table 1.

2. DATA ANALYSIS

All science windows i.e. individual pointings of typical duration between 1500 s and 2000 s have been analyzed for sources in the four energy intervals: 3 – 4, 4 – 8, 8 – 15, and 15 – 25 keV. The analysis software system is OSA–5.1 (Offline Analysis Software) by ISDC (INTEGRAL Science Data Center, Versoix, Switzerland).

The revolutions used for JEM–X2 are: 10, 12, 13, 20-170, 179, 208, 239, 300, 365. The revolutions used for JEMX–1 are: 10, 12, 13, 24, 25, 39-45, 102, 103, 167, 170-252, 255-276, 278-285, 287-295, 300-303, 308-323, 326, 357-360, 365.

The four images produced (one for each energy band) are searched independently for peaks characterized by a detection significance which is the highest peak value divided by the RMS value of the immediate surrounding. A source is accepted if it appears at the same place in at least two of the images with a detection significance larger than 3 or in a single image with a detection significance larger than 10. In total 20,000 source candidates are registrered during the survey of which 1100 are spurious i.e. not identified.

22470 science windows have been searched and source candidates were found in 11071 of those. The catalog was constructed by grouping sources sufficiently close to each other (less than 5′), deriving the average position by weighting with the individual detection significances. The sources included in the JEM–X source catalog are the ones with a position deviation less than 5′from a source in the reference catalog.

3. SOURCE LOCALIZATION ACCURACY

The error of the source localization has a counting statistics and a systematic component. The analysis of Budtz-Jørgensen *et al.* [7] demonstrates a weak dependence on temperature of the satellite structure measured at the mask which is not taken into account in the present anal-

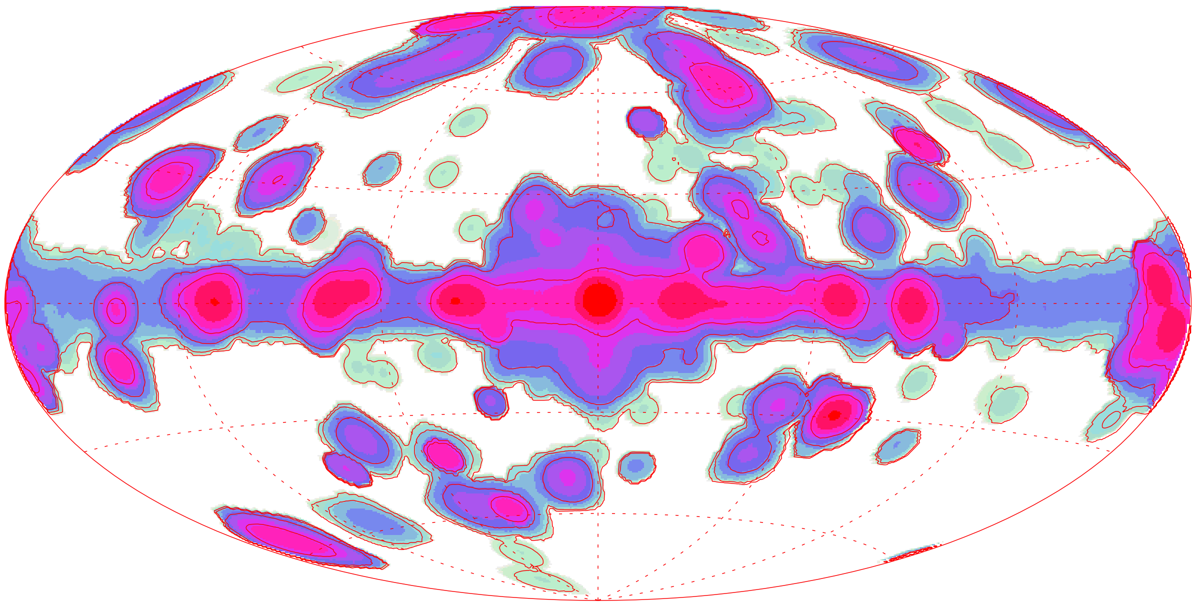

Figure 1. Map in galactic coordinates of exposure time in the science windows used for the present catalog. The contour lines are at 10^2, 10^3, 10^4, and 10^5 s.

ysis. Another effect is the not quite accurate detector response modelling used in the IROS process. Fig. 2 shows the deviation between the found source positions and the reference catalog positions as a function of maximal detection significance for the individual source.

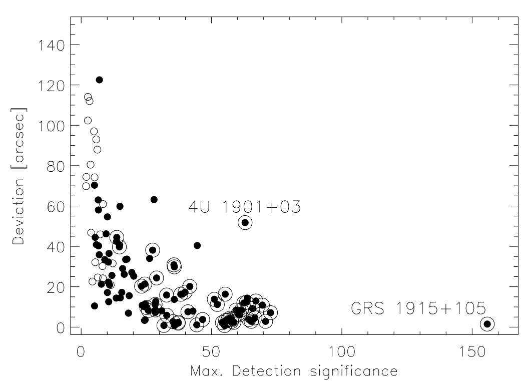

Figure 2. The source position deviation from the reference catalog plotted against the maximal detection significance. The open circles represent sources with one or two detections, the filled circles have more than 2 detections and those that have an extra circle have been detected more than 150 times. GRS 1915+105 is indicated because it has the highest detection significance and 4U 1901+03 is highlighted because the reference catalog position probably is off by ∼40″.

Four sources: IGR J18450-0435, 3EG J1639-4702, AX J1637.8-4656, and AX J1911.0+0906 deviate more than 150″ from the reference catalog position. Each is only detected once so the identification might be questioned and they are subject to further investigation.

On the other hand 4U 1901+03 is a well established source where the JEM–X position deviates ∼40″ from the reference catalog position that perhaps should be revised.

The 2σ confidence limit for source localization in single science windows is defined as the radius that contains 95% of the individual detections in each of four off-axis angle intervals as given in Fig. 3.

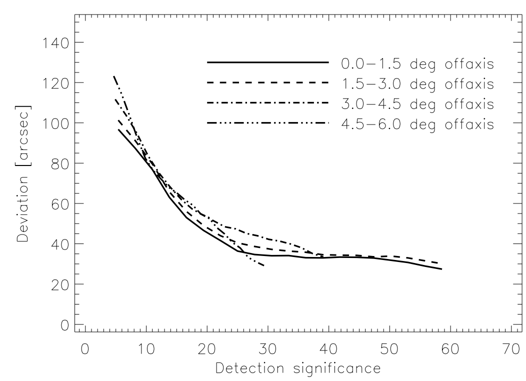

Figure 3. The 95% confidence limits for the localization accuracy determined as a function of the detection significance. The results from four off-axis angle intervals are shown.

4. DETECTION SENSITIVITY

The JEM–X sensitivity has been determined as the lower intensity limit of the identifiable sources. The exposure time was selected to be around 2000 s, which is typical for the INTEGRAL science window durations. Fig. 4 shows the result given in cgs units in the interval where JEM–X is most sensitive (highest effective area).

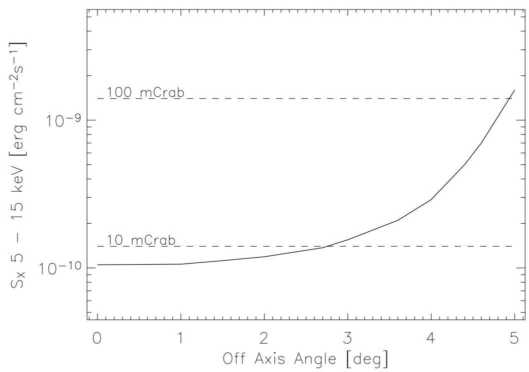

Figure 4. The source detection limit for an observation time of ∼2000 s. The dashed lines gives the comparison with the Crab flux.

5. CRAB NEBULA

The Crab Nebula needs special attention since it is an extended X-ray emitter (see Fig. 5) of diameter of ∼1′. The position is therefore not so well defined and SIMBAD as well as the ISDC reference catalog quote the Crab Pulsar position (RA: 83.6332°, Dec: 22.0145°, J2000).

Since JEM–X is not able to resolve this source the measured position will represent the centroid of the distribution of the emission. As a first approximation to derive that a Chandra image was used (acisf01999N001) as shown in Fig. 5.

The centroid of the Chandra observation excluding the pulsar is at 83.6296°, 22.0182°, whereas the JEM–X position found here is 83.6307°, 22.0176° which is between the Chandra centroid and the pulsar. Hence the reference catalog position is not adequate for an instrument that cannot resolve the nebula.

ACKNOWLEDGEMENTS

Based on observations with INTEGRAL, an ESA project with instruments and science data centre funded by ESA member states (especially the PI countries: Denmark, France, Germany, Italy, Switzerland, Spain), Czech Republic and Poland, and with the participation of Russia and the USA.

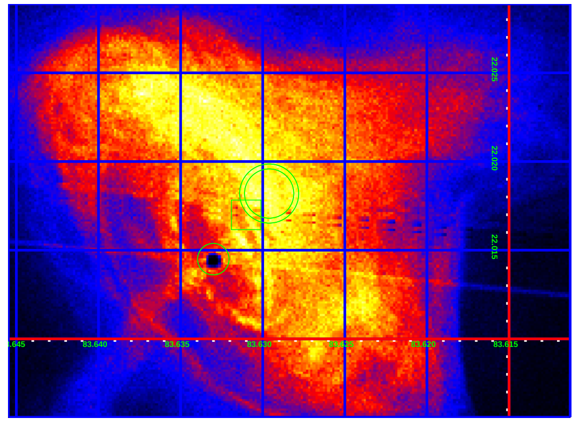

Figure 5. Chandra image of the Crab Nebula. The double ring indicates the position of the centroid of the count distribution. The square is the position of the j_ima_iros position (764 observations) and the smaller circle indicates the pulsar ('Crab' position in the reference catalog).

REFERENCES

[1] Chenevez *et al.*, 2004, ATEL#223.

[2] Chenevez *et al.*, 2006, ATEL#756.

[3] Kuulkers, J. *et al.*, 2006, A&A in preparation.

[4] Lund, N. *et al.*, 2003, A&A, 411, L231.

[5] Ebisawa *et al.*(2003) Astron. & Astrophys. 411, 59.

[6] Bird, A.J., Barlow, E.J., Bassani, L., *et al.*, 2006, ApJ, 636, 765.

[7] Budtz-Jørgensen, C., Lund, N., Westergaard, N.J. *et al.*, 2006, Proc. SPIE Vol. 6266.

6. THE CATALOG

6.1. Description of columns

The sources that are not found in the IBIS catalog [6] are marked with a dagger (†). The dubious sources far from their positions in the reference catalog [5] are marked with an asterisk (∗).

R.A. Right Ascension (J2000) in degrees.

Dec Declination (J2000) in degrees.

Err Error radius (1 σ) in arcmin.

N Number of detections in the entire survey.

Table 1. The JEM–X Catalog

Source name	R.A.	Dec	Err	N
IGR J00291+5934[†]	7.276	59.566	0.39	46
IGR J00370+6122[†]	9.323	61.354	1.51	2
gam Cas	14.211	60.711	1.20	4
SMC X-1	19.271	-73.444	0.49	25
3A 0114+650	19.523	65.283	0.99	5
H 0115+634[†]	19.637	63.744	0.33	59
RX J0146.9+6121[†]	26.744	61.351	1.51	2
NGC 1275[†]	49.946	41.514	0.37	46
EXO 0331+530[†]	53.746	53.176	0.26	123
LMC X-2[†]	80.130	-71.955	0.27	119
LMC X-4	83.219	-66.366	0.25	161
Crab	83.631	22.017	0.18	1038
LMC X-3[†]	84.730	-64.083	0.53	19
LMC X-1[†]	84.935	-69.736	0.26	127
H 0614+091	94.283	9.135	0.72	12
Vela Pulsar	128.844	-45.198	2.13	1
Ginga 0836-429	129.347	-42.892	0.22	251
Vela X-1	135.531	-40.553	0.24	186
H 0918-549	140.112	-55.213	0.81	8
GRO J1008-57	152.450	-58.301	0.44	34
Cen X-3	170.322	-60.625	0.24	205
IGR J11215-5952[†]	170.449	-59.874	0.85	7
HR 4492[†]	174.862	-65.394	1.28	3
IGR J11435-6109[†]	175.975	-61.123	2.13	1
1E 1145.1-6141	176.876	-61.955	0.45	36
H 1145-619	177.020	-62.213	0.66	13
NGC 4151	182.635	39.403	0.28	104
NGC 4388	186.457	12.651	0.93	6
GX 301-2	186.661	-62.770	0.32	90
3C 273	187.277	2.048	0.55	19
3A 1246-588	192.438	-59.113	2.13	1
1H 1254-690	194.404	-69.290	0.47	29
2RXP J130159.5-63580	195.513	-63.961	2.13	1
Cen A	201.365	-43.012	0.30	86
4U 1323-62	201.662	-62.141	0.48	28
IC 4329A	207.338	-30.318	1.00	5
NGC 5506[†]	213.316	-3.217	0.71	10
Cir X-1	230.171	-57.166	0.21	353
H 1538-522	235.594	-52.383	0.27	130
4U 1543-624	236.982	-62.568	0.32	69
XTE J1550-564	237.744	-56.471	0.27	119
1H 1556-605[†]	240.270	-60.738	0.45	30
H 1608-522	243.178	-52.423	0.25	187
Sco X-1	244.979	-15.640	0.28	109
H 1624-490	247.011	-49.198	0.20	508
IGR J16318-4848	247.938	-48.816	1.42	3
IGR J16320-4751	248.020	-47.878	0.63	14
4U 1630-47	248.507	-47.393	0.22	344
AX J1637.8-4656[†*]	249.526	-47.032	2.13	1
3EG J1639-4702[†*]	249.638	-46.937	2.13	1
IGR J16393-4643	249.800	-46.729	2.13	1
H 1636-536	250.231	-53.750	0.21	321
GX 340+0	251.451	-45.612	0.19	652
IGR J16479-4514	252.012	-45.185	2.13	1
GRO J1655-40[†]	253.501	-39.845	0.42	44
OAO 1657-415	255.201	-41.653	0.33	74
GX 339-4	255.707	-48.790	0.24	210
4U 1700-377	255.987	-37.844	0.24	194
GX 349+2	256.437	-36.424	0.21	366
H 1702-429	256.561	-43.035	0.30	101
H 1705-440	257.226	-44.102	0.24	237
XTE J1709-267	257.368	-26.652	1.51	2
IGR J17098-3628[†]	257.421	-36.447	2.13	1
Oph Cluster	258.081	-23.356	2.13	1
4U 1708-40	258.094	-40.841	0.52	22
XTE J1716-389	258.964	-38.856	1.51	2
XTE J1720-318	259.995	-31.751	0.43	33
4U 1722-30	261.889	-30.804	0.23	228
3A 1728-169	262.935	-16.962	0.25	173
GX 354-0	262.989	-33.834	0.19	762
GX 1+4	263.011	-24.747	0.24	205
4U 1730-335	263.355	-33.390	0.26	145
SLX 1735-269	264.575	-26.997	0.66	23
4U 1735-444	264.742	-44.450	0.24	191
IGR J17391-3021	264.794	-30.337	1.24	5
SLX 1737-282	265.171	-28.298	2.13	1
XTE J1743-363	265.796	-36.370	2.13	1
1E 1740.7-2942	265.989	-29.753	0.25	156
1A 1742-294	266.528	-29.519	0.21	332
IGR J17464-3213	266.565	-32.233	0.19	781
1A 1743-288	266.761	-28.883	0.26	138
SLX 1744-299	266.858	-30.017	0.31	72
GX 3+1	266.986	-26.564	0.18	1646
SLX 1746-331[†]	267.452	-33.202	0.28	132
1H 1746-370	267.553	-37.051	0.25	175
GRS 1747-312	267.690	-31.276	0.46	30
IGR J17544-2619	268.608	-26.344	1.56	2
GX 5-1	270.286	-25.077	0.18	1233
GRS 1758-258	270.300	-25.742	0.62	15
GX 9+1	270.384	-20.530	0.21	471
GX 13+1	273.630	-17.158	0.22	317
4U 1812-12	273.756	-12.098	1.25	3
GX 17+2	274.005	-14.036	0.21	343
H 1820-303	275.918	-30.359	0.21	358
AX J1824.7-1253[†]	276.194	-12.900	2.13	1
H 1822-000	276.340	-0.011	0.29	94
3A 1822-371	276.446	-37.104	0.29	93
Ginga 1826-24	277.367	-23.796	0.27	128
Ser X-1	279.988	5.036	0.21	366
IGR J18410-0535	280.259	-5.601	1.54	2
IGR J18450-0435[*]	281.241	-4.546	1.68	2
Ginga 1843+009	281.384	0.868	0.82	8
IGR J18483-0311	282.057	-3.164	1.57	2
3A 1850-087	283.261	-8.696	1.25	3
XTE J1855-026	283.873	-2.606	0.62	14
XTE J1858+034	284.678	3.436	0.33	78
4U 1901+03	285.913	3.204	0.22	247
H 1907+097	287.400	9.833	0.33	77
AX J1910.7+0917[†]	287.676	9.279	2.13	1
4U 1909+07	287.698	7.593	0.53	20
AX J1911.0+0906[†*]	287.737	9.053	1.51	2
Aql X-1	287.816	0.584	0.26	169
SS 433	287.946	4.986	0.30	86
IGR J19140+0951	288.512	9.881	0.82	9
GRS 1915+105	288.798	10.946	0.18	853
4U 1916-053	289.696	-5.234	0.27	113
KS 1947+300	297.400	30.206	0.98	7
3A 1954+319[†]	298.919	32.088	1.04	6
Cyg X-1	299.586	35.202	0.21	345
4U 1957+115[†]	299.853	11.713	1.58	2
EXO 2030+375	308.063	37.638	0.29	122
Cyg X-3	308.106	40.957	0.19	696
SAX J2103.5+4545	315.892	45.753	0.33	67
SS Cyg	325.693	43.590	1.35	3
Cyg X-2	326.168	38.320	0.28	124
3A 2206+543	331.979	54.519	1.21	4
Cas A	350.860	58.818	0.20	364